Article

Molecular Cell

Coordinated Activity of Y Family TLS Polymerases and EXO1 Protects Non-S Phase Cells from UV-Induced Cytotoxic Lesions

Graphical Abstract

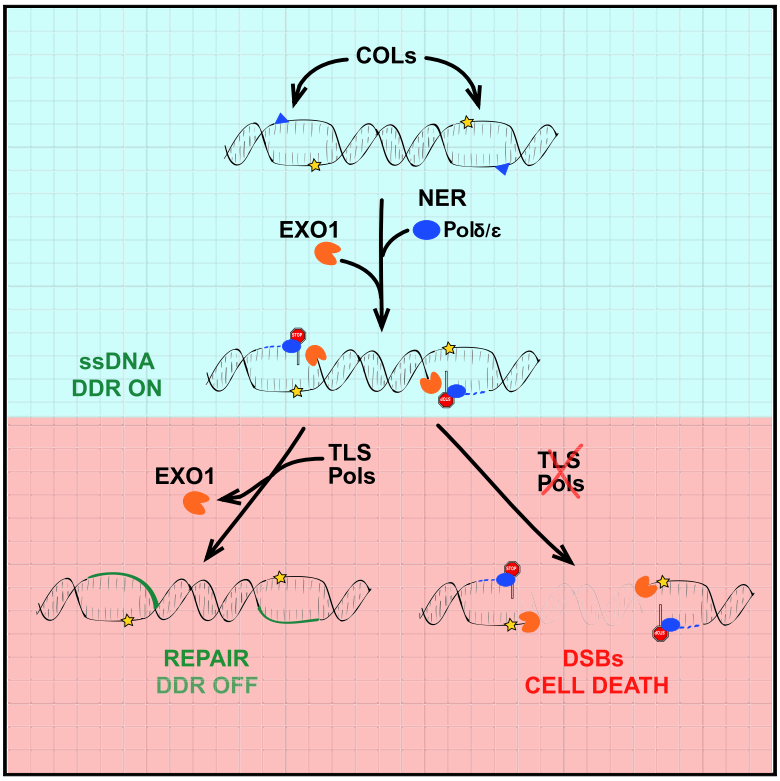

Authors

Sarah Sertic, Antonio Mollica, Ilaria Campus, Stefania Roma, Emanuela Tumini, Andrés Aguilera, Marco Muzi-Falconi

Correspondence

sarah.sertic@unimi.it (S.S.), marco.muzifalconi@unimi.it (M.M.-F.)

In Brief

Sertic et al. investigate how non-replicating cells repair UV-induced DNA lesions. Repair of problematic lesions by nucleotide excision repair involves EXO1 and TLS polymerases. These enzymatic activities are critical to allow proper DNA damage checkpoint signaling and effective DNA repair and to prevent formation of cytotoxic DNA breaks.

Highlights

- Closely opposing lesions (COLs) are problematic for NER
- EXO1 processes COLs and recruits TLS polymerases
- TLS polymerases are required to complete repair synthesis
- Balance of EXO1/TLS Pols modulates checkpoint response and prevents DSBs

Sertic et al., 2018, Molecular Cell *70*, 34–47
April 5, 2018
https://doi.org/10.1016/j.molcel.2018.02.017

CellPress

CellPress

Molecular Cell
Article

Coordinated Activity of Y Family TLS Polymerases and EXO1 Protects Non-S Phase Cells from UV-Induced Cytotoxic Lesions

Sarah Sertic,[1,*] Antonio Mollica,[1] Ilaria Campus,[1] Stefania Roma,[1] Emanuela Tumini,[2] Andrés Aguilera,[2] and Marco Muzi-Falconi[1,3,*]

[1]Dipartimento di Bioscienze, Università degli Studi di Milano, Via Celoria 26, 20133 Milano, Italy
[2]Universidad de Sevilla-CSIC-Universidad Pablo de Olavide, Seville 41092, Spain
[3]Lead Contact
*Correspondence: sarah.sertic@unimi.it (S.S.), marco.muzifalconi@unimi.it (M.M.-F.)
https://doi.org/10.1016/j.molcel.2018.02.017

SUMMARY

UV-induced photoproducts are responsible for the pathological effects of sunlight. Mutations in nucleotide excision repair (NER) cause severe pathologies characterized by sunlight sensitivity, coupled to elevated predisposition to cancer and/or neurological dysfunctions. We have previously shown that in UV-irradiated non-cycling cells, only a particular subset of lesions activates the DNA damage response (DDR), and this requires NER and EXO1 activities. To define the molecular mechanism acting at these lesions, we demonstrate that Y family TLS polymerases are recruited at NER- and EXO1-positive lesion sites in non-S phase cells. The coordinated action of EXO1 and Y family TLS polymerases promotes checkpoint activation, leads to lesion repair, and is crucial to prevent cytotoxic double-strand break (DSB) formation.

INTRODUCTION

UV light, a genotoxic agent to which we are exposed daily, generates mainly cyclobutane pyrimidine dimers (CPD) and 6,4 photoproducts (6-4PP). These lesions represent a paradigm for all DNA distorting bulky adducts (Friedberg, 2001) and are responsible for the pathological effects of sunlight. In healthy organisms, helix-distorting lesions are removed by nucleotide excision repair (NER) (Spivak, 2015). Mutations in NER genes cause the onset of human pathologies like xeroderma pigmentosum (XP), Cockayne syndrome (CS), trichothiodystrophy (TTD), and UV-sensitive syndrome (UVSS). A common hallmark of these diseases is a strong sensitivity to UV; however, other syndrome-specific phenotypes, such as high predisposition to tumors development in XP or neurological dysfunctions in both XP and CS patients have been reported (Lehmann, 2003; Schärer, 2013).

To ensure genome integrity, following DNA damage, cells activate a DNA damage response (DDR) (Harper and Elledge, 2007).

Previous works demonstrated that the checkpoint response following UV irradiation cannot be activated directly by the lesions *per se,* but it requires NER function. Indeed, yeast strains mutated in NER and human fibroblasts derived from XP patients fail to activate the DDR outside S phase (Giannattasio et al., 2004; Marini et al., 2006; Marti et al., 2006; O'Driscoll and Jeggo, 2003).

During S phase, UV lesions block replicative DNA polymerase activities, and completion of chromosome duplication is possible thanks to the intervention of specialized translesion synthesis (TLS) polymerases (Sale et al., 2012). While these enzymes have been characterized in their chromosome replication role, evidence begins to accumulate that suggest their involvement in DNA repair mechanisms.

Understanding the mechanism(s) connecting removal of bulky lesions from DNA to checkpoint activation independently of replication will be of clinical relevance because most human cells are not replicating, post-mitotic, or terminally differentiated (e.g., keratinocytes, adipocytes, and neurons).

NER is a multistep process where the adduct-containing DNA is incised 5′ and 3′ to the lesion, and the resulting gap (~30 nt) is refilled by repair DNA synthesis (Schärer, 2013). The polymerases that execute this step are Polδ and Polε, and more recently, a role for Polκ was also reported (Ogi and Lehmann, 2006; Ogi et al., 2010). Mechanistic insights and how these polymerases divide their labor are not clear yet. A variation on the canonical NER mechanism in *E. coli* has been originally proposed based on the identification of repair products where unscheduled DNA synthesis covers a "long patch" as opposed as the canonical short patch (Cooper and Hanawalt, 1972). The molecular details of this "long patch NER" and the DNA polymerase activities involved are still lacking.

Polκ is a member of the Y DNA polymerase family, which also includes Polι, Polη (XP-V), and REV1. These enzymes, whose function is coordinated through PCNA ubiquitylation, possess unique features that enable them to synthesize DNA copying a template containing a variety of lesions but at the same time, make them highly mutagenic (Vaisman and Woodgate, 2017). A tight control over their activity is crucial for the maintenance of genomic integrity.

Ogi and Lehmann (2006) and Ogi et al. (2010) demonstrated that also in quiescent mammalian cells PCNA is ubiquitylated after UV irradiation and showed that Polκ is recruited at UV-induced damaged sites through a NER-dependent

mechanism, which is very similar to what has been reported for EXO1 (Sertic et al., 2011).

We previously demonstrated that EXO1 nuclease (Tran et al., 2004) plays a crucial role in processing a subset of "problematic" UV-induced lesions and in triggering the DDR. In particular, when the gap-refilling step of NER cannot be promptly completed, EXO1 gains the kinetic opportunity to process the stalled intermediate and generate long tracks of ssDNA, providing the alert signal for checkpoint activation both in yeast and human non-cycling cells (Giannattasio et al., 2010; Sertic et al., 2011). The role of EXO1 in UV-induced checkpoint activation *in vivo* has been recently supported by *in vitro* reconstitution of the activation pathway with purified components from human cells (Lindsey-Boltz et al., 2014).

UV-induced closely spaced opposing lesions (COLs) may represent the "problematic" intermediate. Indeed, removal of one of the lesions by NER would leave the second lesion in the complementary strand in a single-stranded DNA (ssDNA) configuration, which cannot be further processed by NER nucleases until the double-stranded DNA (dsDNA) configuration is reestablished (Svetlova et al., 2002; Svoboda et al., 1993). The persisting lesion, in the template strand, blocks gap refilling through repair DNA synthesis by Polδ/ε. Targeting of this gapped intermediate by EXO1 leads to activation of the checkpoint, signaling a problematic repair. Reconstitution of the double helix in this tract would quench the checkpoint response, but would require the involvement of translesion synthesis (TLS) polymerases to copy the lesion-containing template strand. Intriguingly, COLs resemble interstrand crosslinks (ICLs), whose processing mechanism include multiple DNA repair and DNA damage tolerance pathways such as NER and TLS polymerases (reviewed in Muniandy et al., 2010). In addition, a replication-independent repair (RIR) mechanism for ICLs has been reported in yeast and in mammalian cells that relies on Polζ and Polκ respectively (Sarkar et al., 2006; Williams et al., 2012) .

Here, we show that in human cells, Polκ and Polι are recruited to local UV-damaged sites together with and depending on EXO1, suggesting that their role in NER mechanism may be to intervene in repair synthesis at COLs. Moreover, we demonstrate that maintaining a controlled balance between TLS polymerases and EXO1 nuclease is crucial for the functional resolution of a subset of UV-induced damages, for the proper response to UV irradiation and for prevention of UV-induced DSBs in non-cycling cells. Indeed, inhibiting repair synthesis or TLS polymerase recruitment leads to a hyper-activation of the checkpoint and to a degeneration of UV-induced lesions into DSBs through uncontrolled EXO1 activity.

RESULTS

Y Family TLS Polymerases Are Recruited at EXO1-Positive Local UV Damage Sites

Y family TLS polymerases are specialized enzymes with a more relaxed active site that accounts for their ability to bypass different DNA lesions on the template strand (Goodman and Woodgate, 2013) in either error-free or error-prone pathways (reviewed in Guo et al., 2009). We have shown that EXO1 is recruited at a subset of UV lesions, which are deemed to be problematic to repair (Sertic et al., 2011); previous work reported that Polκ plays a partial role in NER-dependent repair synthesis (Ogi et al., 2010). To verify whether Polκ and possibly other TLS polymerases from the Y family may be acting at the same problematic lesions where EXO1 is recruited, we generated local UV damage (LUD) (Volker et al., 2001) and monitored proteins that are recruited at LUD sites. Cells expressing eGFP-tagged versions of Polκ, Polι, Polη, and REV1 (Figure S1) were co-transfected with an EXO1-mCherry construct. Figure 1A shows that, following local UV irradiation, all Y family polymerases are recruited at EXO1-positive LUDs. The fluorescence intensity measured along a line across LUDs for each Y-TLS Pols, EXO1 and XPA shows the same profile (Figure 1B), supporting colocalization. We validated the selective recruitment of Y family TLS polymerases by showing that eGFP-POLν (A-family polymerase), used as a negative control, did not accumulate at LUDs (Figure S2A). Nearly 50% of the NER-positive LUDs were also positive for EXO1, which is found at LUDs only in non-S phase cells (Sertic et al., 2011). Interestingly, Polκ and Polι are only recruited to EXO1-positive LUDs (Figure 1C), suggesting that Polκ and Polι, as was previously shown for EXO1, are only acting at a subset of lesions in non-replicating cells. On the other hand, Polη and REV1 are found at nearly 80% of NER-positive LUDs, of which only half was also EXO1-positive (Figure 1C).

Therefore, Polκ and Polι are specifically recruited at EXO1-positive sites after UV treatment, while Polη and REV1 have a wider distribution that could be explained by their broader spectrum of roles, such as their recruitment in S phase cells at replication factories and stalled replication forks (Kannouche and Lehmann, 2004; Kannouche et al., 2001).

These results were further strengthened by labeling cells with 5-ethynyl-2'-deoxyuridine (EdU) after UV irradiation, which is incorporated by both replicative and repair synthesis machineries, albeit to a different extent. This procedure allows us to clearly distinguish S phase from non-S phase cells. As expected, while EXO1, Polκ, and Polι are recruited to LUDs in non-S phase cells, Polη and REV1 are also found at LUDs in S phase cells (Figures S2B and S2C).

EXO1-Dependent Processing Promotes Polκ and Polι Recruitment

To investigate if EXO1 presence and activity is required for the recruitment of TLS Pols at UV lesions, we produced EXO1$^{-/-}$ clones exploiting the CRISPR-Cas9 technology using two different guide RNAs (gRNAs) (EXO1$^{-/-}$.3 and EXO1$^{-/-}$.15) and a gRNA against Luciferase as a control (CTR). To check for gRNA specificity, we Sanger-sequenced two genes with the highest score in the off-target list created by the algorithm in Singh et al. (2015) for each target sequence, and we did not detect any InsDels (Figure S3A). EXO1 KO clones were confirmed by Sanger-sequencing the EXO1 genomic locus (data not shown) and absence of protein was verified by immunoprecipitation (Figure S3B). Significant cell-cycle alterations in the KO clones were excluded by cytofluorimetric analysis (Figure S3C).

If TLS polymerases accumulated at EXO1-processed lesions, we expected to see a defective recruitment in EXO1$^{-/-}$ clones. For this purpose, EXO1 KO and control clones were transfected

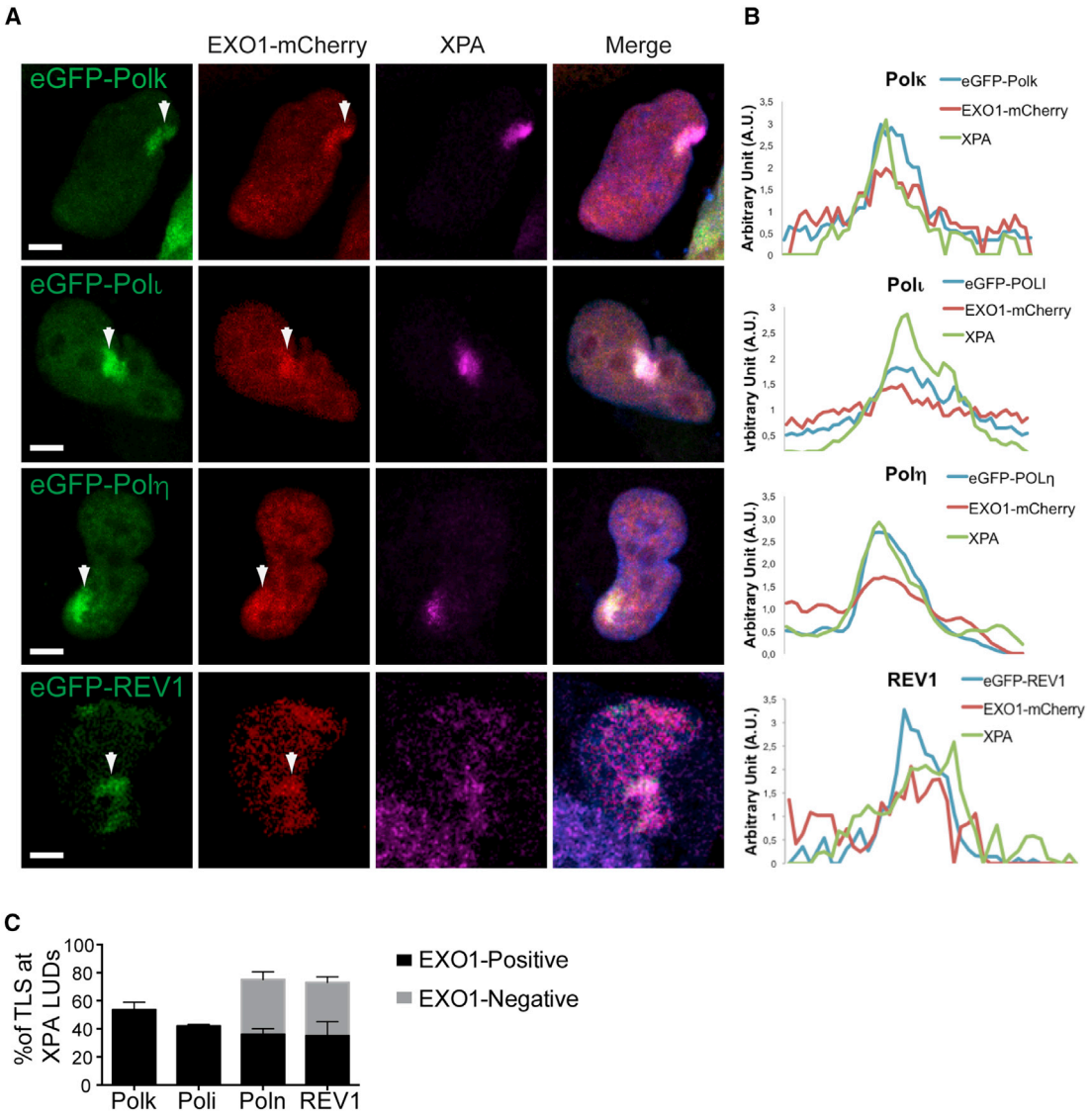

Figure 1. TLS DNA Polymerases κ and ι, but Not η and REV1, Are Recruited Exclusively to EXO1-Positive LUDs

(A) MRC5VI cells were transfected with eGFP and mCherry tagged constructs, locally UV irradiated at 100 J/m^2, incubated for 1 hr, and processed for immunofluorescence with anti-XPA antibody. A representative example of one LUD for each condition is shown. Arrowheads point to LUDs. Scale bar, 5 μm.

(B) Fluorescence intensity across LUDs was measured using ImageJ. Graphs indicate fluorescence intensity variations expressed as a.u.

(C) XPA-positive LUDs were scored for TLS polymerases and EXO1. 20 LUDs were analyzed in each experiment for each condition. At least three independent experiments were performed. Error bars, ±SEM.

with constructs expressing eGFP-Polκ, -Polι, -Polη, and -REV1. Cells were locally UV-irradiated and immunostained for either XPA or XPB (plotted as NER factors). Representative images are shown in Figure 2A. LUDs positive for NER factors were counted and scored as positive or negative for TLS enzymes as indicated in Figure 2B. Polκ, Polι, Polη, and REV1 are recruited at LUDs in control cells at a percentage nearly 70%, 60%, 86%, and 88%, respectively. Strikingly, we observed that, while Polη and REV1 efficiently localize at damage sites also in EXO1$^{-/-}$ clones, Polκ and Polι recruitment is nearly abolished in the absence of EXO1 (Figure 2B). To exclude that such differences in Pols recruitment may be linked to variations in expression between EXO$^{+/+}$ and EXO$^{-/-}$ cells, we verified that Polκ, Polι, Polη, and REV1 are expressed at similar levels in EXO1 KO clones compared to CTR cells (Figures S4A and S4B).

Importantly, complementation of EXO1 KO clones with EXO1-mCherry restores Polκ and Polι recruitment (Figures 2C and 2D, images and quantification, respectively). On the contrary, complementation of LUC and EXO1$^{-/-}$ clones with an EXO1-D173A-mCherry mutant lacking EXO1 catalytic activity (Bregenhorn and Jiricny, 2014) dramatically reduces the accumulation of Polκ and Polι at LUDs (Figure 2D). This observation indicates that EXO1-dependent processing of the gap is responsible for the recruitment of Y family polymerases.

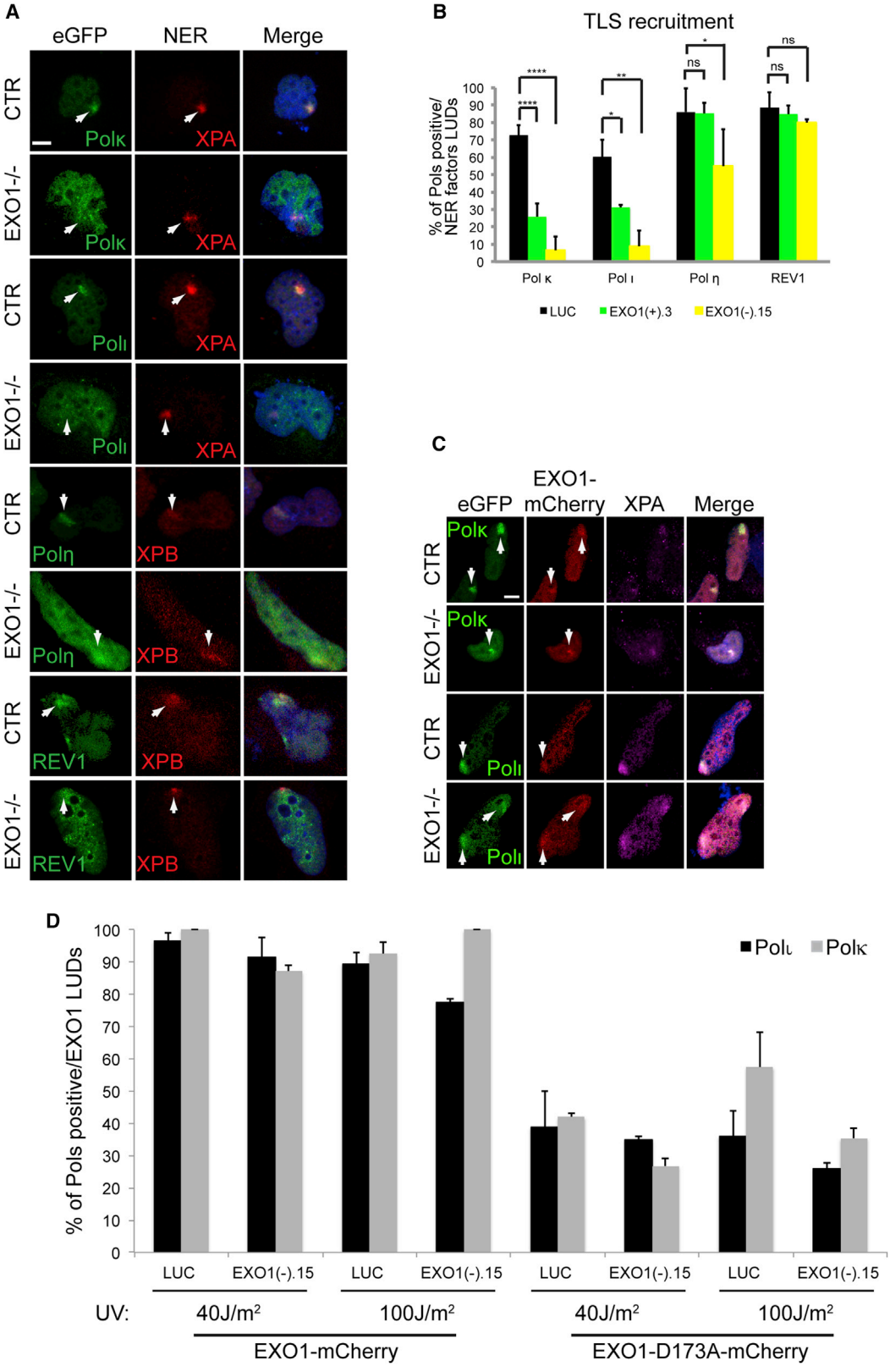

(legend on next page)

When we characterized the EXO1-D173A mutant, we noticed that nuclease defective EXO1 is loaded at LUDs but its recruitment is transient compared to active EXO1 (Figure S4C). The inactive form of EXO1 becomes more persistently localized at LUDs if DNA polymerase activity is inhibited by adding 1-β-D-arabinofuranosylcytosine (AraC) immediately after UV irradiation (Figure S4C). These observations support the notion that gap refilling competes with gap enlargement. If EXO1 is present but inactive, DNA polymerases fill the gap and displace EXO1 from DNA. On the other hand, if gap refilling is prevented by inhibiting DNA polymerases, the inactive form of EXO1 remains stably associated to damaged DNA.

Repair Synthesis Inhibition Increases Polκ, Polι, Polη, and REV1 Recruitment

COLs might be seen as "problematic" damages because the template strand lesions can hamper repair synthesis. We can expand the fraction of "problematic" lesions by either increasing the UV dose or by inhibiting repair DNA polymerases. Under these conditions, EXO1 recruitment at LUDs is strongly enhanced (Sertic et al., 2011). Thus, we asked whether inhibition of normal repair synthesis acts as a signal for the recruitment of TLS polymerases at repair intermediates. We tested how recruitment of Polκ, Polι, Polη, and REV1 at LUDs is affected by addition of AraC at low UV fluencies, a condition where all lesions are seen as "problematic" (Sertic et al., 2011). Figure 3 shows that generating LUDs at 40 J/m^2 leads to a recruitment of Y family polymerases at a fraction of NER-positive LUDs, as previously shown for EXO1 (Sertic et al., 2011). Upon treatment with AraC right after UV irradiation, the percentage of TLS Pols-positive LUDs increased 2.1×, 1.7×, 1.7×, and 1.7× for Polκ, Polι, Polη, and REV1, respectively. A similar increase can be measured by irradiating with a higher UV dose (100 J/m^2). At this high fluency, AraC had only a mild effect on TLS enzymes recruitment, likely because of saturation effects due to the number or type of lesions induced, as previously observed for RPA in similar experimental conditions (Overmeer et al., 2011). We conclude that an increase in the number of "problematic" lesions, obtained by blocking repair synthesis or raising UV dosage, promotes the recruitment of Polκ, Polι, Polη, and REV1.

Gap-Refilling Inhibition Enhances Checkpoint Activation and Lesions Degeneration

We have shown in quiescent primary cells that EXO1-dependent ssDNA-gapped intermediates are required to efficiently trigger ATR (Sertic et al., 2011). EXO1-dependent gap formation and DNA polymerase-dependent gap refilling are in competition (Giannattasio et al., 2010; Sertic et al., 2011). Therefore, we hypothesized that gap refilling by DNA polymerases may be important to modulate the DDR by quenching checkpoint signaling.

To verify this hypothesis, we initially inhibited gap-refilling activity with AraC and monitored checkpoint activation. Primary fibroblasts were serum-starved to deplete S phase cells (0.4% of cells were still replicating in our experimental conditions, Figure S5A). We UV-irradiated cells in the absence or presence of AraC and monitored DDR markers at different time points. One hour after treatment, UV-irradiated cells exhibited p53 ser15 phosphorylation, which was greatly enhanced if cells were exposed to AraC, whereas γH2AX was barely detectable (Figure 4A). UV irradiation of non-cycling cells also induced PCNA mono-ubiquitylation (PCNA-mUb) and AraC exposure clearly increased it (Figure 4A, see graph for quantification).

Figures 4B and 4C show that, at later time points, an even higher p-p53 ser15 accumulation was evident. Moreover, in cells treated with UV and AraC, we also observed a significant γH2AX increase, as previously observed by Matsumoto et al. (2007).

Surprisingly, UV-irradiated cells, where gap refilling was prevented by AraC exposure, exhibited a very strong phosphorylation of RPA32 at serine 4/8 (Figure 4B). This marker is specific for DSB-activated DNA-PK (Cruet-Hennequart et al., 2006).

In fact, the DNA-PK activated form (p-ser2056) was found at LUDs in a large fraction of cells, following UV+AraC treatment. In the absence of AraC, the activation of DNA PK is reduced (Figures 4D and 4E).

On the contrary, PCNA mono-ubiquitylation, which is not involved in DSB processing, started to decrease 5 hr and, more evidently, 24 hr after treatment with UV and AraC (Figure 4B).

Altogether, these results confirm gap refilling leads to quenching of the checkpoint response and possibly protects cells from the formation of unscheduled DSBs.

Impairment of TLS Recruitment Enhances UV-Induced EXO1-Dependent DSB Formation and Checkpoint Activation

Our results indicate that when repair synthesis cannot rapidly close the NER-dependent gap, EXO1 processes the repair intermediate, and TLS polymerases are recruited to overcome the DNA synthesis block. To test this model, we analyzed the involvement of Polκ in taking care of these problematic lesions

Figure 2. Recruitment of DNA Polymerase κ and ι at LUDs Is EXO1 Dependent

MRC5VI EXO1$^{+/+}$ (CTR) and MRC5VI EXO1$^{-/-}$ (.3 and 0.15 clones) were transfected with constructs expressing eGFP-tagged TLS polymerases as indicated. Cells were locally UV irradiated with 100 J/m^2, incubated for 1 hr, and processed for fluorescence microscopy. XPA and XPB were visualized with specific antibodies.

(A) Representative images of LUDs in each condition tested. Arrowheads point to LUDs. Scale bar, 5 μm.

(B) At least 40 LUDs (positive for XPA or XPB) were analyzed for each condition for each of three independent experiment and scored for presence or absence of TLS polymerase. Student's t test was performed: *p value < 0.05; **p value < 0.005; ****p value < 0.0001. ns, not statistically significant. Error bars, ±SEM.

(C) MRC5VI EXO1$^{+/+}$ (CTR) and MRC5VI EXO1$^{-/-}$ (.15 clones) were transfected with eGFP-tagged Polκ and Polι and EXO1-mCherry constructs. Cells were locally UV irradiated at 100 J/m^2, incubated for 1 hr, and processed for immunofluorescence. Representative images of LUDs are shown on the left. Arrowheads point to LUDs.

(D) MRC5VI EXO1$^{+/+}$ (LUC) and MRC5VI EXO1$^{-/-}$ (.15 clones) were transfected with eGFP-tagged Polκ and Polι and EXO1-mCherry or EXO1-D173A-mCherry constructs. Cells were locally UV irradiated at 40 or 100 J/m^2 and incubated for 1 hr. AraC was added to after irradiation (see text). At least 25 LUDs were scored for each condition in all three independent experiments and plotted on the graph. Error bars, ±SEM.

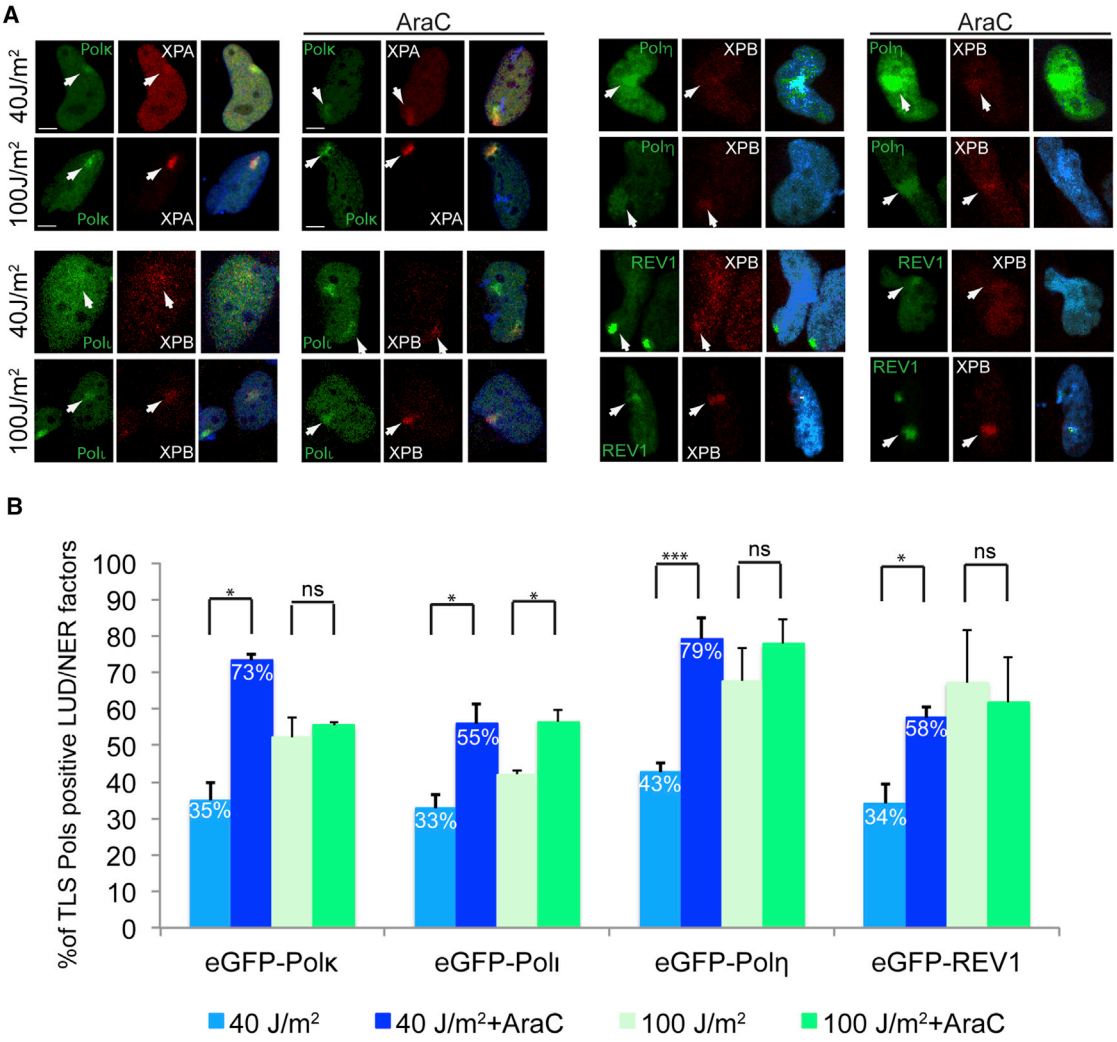

Figure 3. Polκ, Polι, Polη, and REV1 Are Recruited to LUDs when DNA Repair Synthesis Cannot Be Completed

(A) MRC5VI cells were transfected with the indicated eGFP-TLS polymerase constructs. Cells were locally UV irradiated at 40 or 100 J/m^2 in the presence or absence of AraC. Representative images for each condition are shown. Scale bar, 5 μm.

(B) At least 40 XPA- or XPB-positive LUDs for each condition were scored for recruitment of Polκ, Polι, Polη, and REV1. Student's t test was performed: *p value < 0.05; ***p value < 0.001. ns, not statistically significant. Error bars, ±SEM.

by monitoring how Polκ contributes to quenching the UV checkpoint response in non-S phase cells. We serum-starved 48BR primary human fibroblasts and we silenced Polκ expression with a pool of siRNAs (the individual siRNAs are shown in Figure S5B). Cells were then UV-irradiated and harvested at different time points. Both p-p53 ser15 and γH2AX checkpoint markers indicate that depletion of Polκ leads to a hyperactive checkpoint response at 5 hr post UV-irradiation (Figures 5A, 5B, and S5C).

In G_0–G_1 cells, the major DSB repair pathway is non-homologous end joining (NHEJ), which is promoted by DNA-PK. In order to establish whether Polκ protects UV-irradiated cells from the formation of deleterious DSBs, we monitored whether the active form of DNA-PK (Chen et al., 2005) is found at LUDs when repair synthesis and EXO1 activity are unbalanced as a consequence of downregulating Polκ. Figures 5C and 5D show that in the absence of the protective role of Polκ, phosphorylated DNA-PK accumulates at LUDs, indicating that UV lesions are being converted to DSBs.

To test the possible contribution of other Y family polymerases at "problematic" lesions, we prevented their recruitment at LUDs through downregulation of the RAD18 E3-ubiquitin ligase to abolish UV-induced PCNA mono-ubiquitylation on K164 (Andersen et al., 2008; Bienko et al., 2005; Hoege et al., 2002; Kannouche and Lehmann, 2004). RAD18 knockdown was confirmed by RT-PCR and western blotting (Figures S5D and S5E) and subsequently by monitoring PCNA mono-ubiquitylation levels on Lys164. Figure 5E confirms that siRAD18 cells fail to achieve proper PCNA-mUb following UV irradiation and shows that p-p53-ser15 and γH2AX modifications are

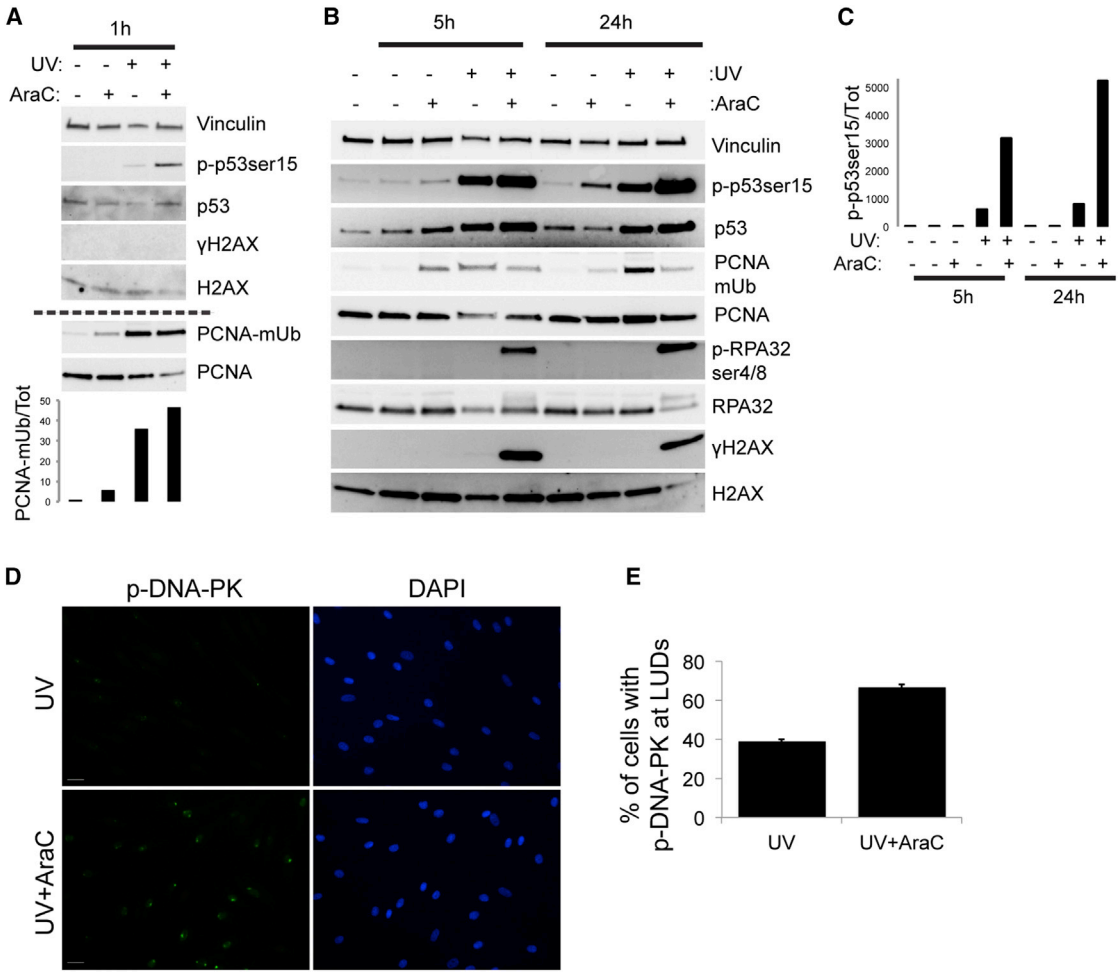

Figure 4. DDR Is Hyperactivated When Repair Synthesis Is Impaired

(A and B) 48BR fibroblasts were serum starved for 72 hr. Cells were subsequently treated with or without AraC and UV (20 J/m^2). Cells were then harvested at the indicated time points and analyzed by SDS-PAGE and immunostained as indicated. (A) shows checkpoint markers 1 hr after irradiation. (B) shows checkpoint markers 5 hr and 24 hr after irradiation.

(C) Quantification was performed with Volume Tool in ImageLab Software; p-p53 ser15 bands normalized to total p53 are represented.

(D) 48BR cells were serum starved for 72 hr, LUDs were generated at 100 J/m^2, and cells were re-incubated for 5 hr followed by immunostaining as indicated. Images were acquired with a 20× objective (N.A. = 0.5). Scale bar, 30 μm.

(E) Quantification was performed counting 150–200 cells for each condition. Two independent experiments were performed. Error bars, ±SEM.

anticipated and enhanced in cells silenced for RAD18 compared to control cells. Intriguingly, we observed a strong RPA32 ser4/8 phosphorylation when TLS recruitment was impaired by RAD18 silencing (Figure 5E) similarly to what was reported in Figure 4B following inhibition of repair synthesis with AraC. RPA32 ser4/8 phosphorylation, a proxy for DSBs, is lost in siRAD18 cells where EXO1 is concomitantly downregulated (Figure 5F), supporting the hypothesis that conversion of "problematic" UV lesions to DSBs is promoted by EXO1 and counteracted by TLS polymerases. Accordingly, siRAD18 cells accumulate p-DNA-PK ser2056-positive LUDs (Figures 5G and 5H). Strikingly, silencing RAD18 in NER-deficient cells (XP-A) did not induce p-DNA-PK ser2056 accumulation at LUDs (Figures 5G and 5H) similarly to what was reported for EXO1 recruitment (Sertic et al., 2011).

These observations strongly suggest that DSBs are created after UV irradiation as a consequence of a failed gap refilling by Y family TLS polymerases.

To test this hypothesis, we analyzed DSBs formation by neutral comet assay, using UV-irradiated cells silenced for RAD18 or non-silenced as control cells. Bleocin, a known DSB-inducing agent was used as positive control. A representative image for each sample is shown at the top of Figure 5I, and tail moment measurements are reported as a graph (Figure 5I, right panel). UV irradiation, per se, did not lead to significant levels of DSBs formation. When TLS polymerases recruitment is prevented by silencing RAD18, we observed a dramatic increase of DSBs (compare the tail moment in siRAD18 and siLUC UV-irradiated cells in Figures 5I and S5F). Intriguingly, in these conditions, DSBs formation is dependent upon EXO1, indeed,

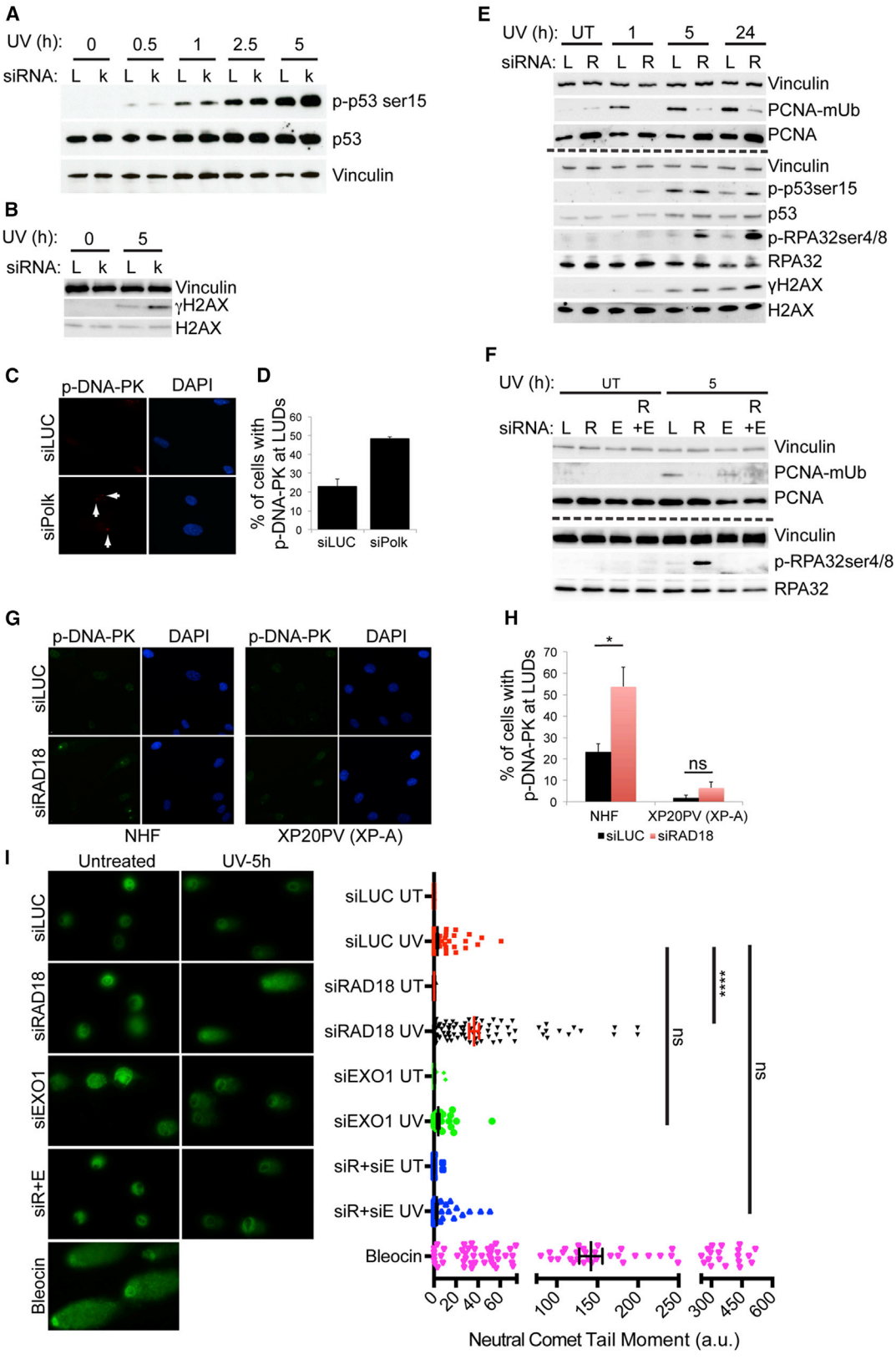

(legend on next page)

DSBs formation is prevented in siRAD18 cells if EXO1 is silenced as well.

Differential Contribution of Y Family Polymerases to the Repair of a Subset of UV-Induced Lesions

The observations reported above complement those previously reported (Ogi et al., 2010) and show that Polκ is involved in NER-dependent repair of a subset of "problematic" UV-induced lesions. However, the results obtained by silencing RAD18 suggested that Polη, Polι, and REV1 may also participate in this process in non-cycling cells, contributing to modulation of checkpoint signaling and protection from DSBs formation (Figure 5).

To evaluate Polη contribution to the checkpoint response after UV in non-cycling cells, we initially silenced Polκ in 48BR fibroblasts and XP-V, which are mutated in Polη. We observed an increase of RPA ser4/8 phosphorylation and γH2AX accumulation compared to cells lacking Polκ only (Figure S6A).

We thus analyzed the contribution of each Y family DNA polymerase to repair DNA synthesis. Serum-starved primary cells were silenced for each Y family polymerases or simultaneously for all four (Figure S6B). DNA repair synthesis (unscheduled DNA synthesis [UDS]) following 20 J/m^2 UV irradiation was analyzed by incubating cells for 2 hr with EdU. Newly synthesized DNA was then labeled by Click-IT (see the STAR Methods) and cells were analyzed by fluorescence microscopy (Limsirichaikul et al., 2009; Sertic et al., 2011). Figure 6A shows that silencing Polκ results in a drastic reduction in repair synthesis, similarly to what was reported previously (Ogi et al., 2010), while all other polymerases contributed only partially to UDS.

We then examined how members of Y family polymerases participated to protecting UV lesions from being converted to DSBs. We measured tail moments in neutral comet assays in silenced cells exposed to UV light, as above. Polκ and Polι are recruited when, during the enlargement of the gap, EXO1 exposes different types of lesions on the ssDNA template strand complexed with RPA. In agreement with the UDS results, Polκ-silenced cells exhibited elevated tail moments that were not significantly different from those measured in RAD18-silenced cells. Individual silencing of Polη-, Polι-, and REV1 led to formation of lower amounts of DSBs (Figure 6B). As expected, DSB generation due to downregulation of Polκ is similar to that observed following simultaneous silencing of all Y family Pols (Figures 6C and S6C).

To verify a possible redundancy between Polη, Polι, and REV1, we silenced all three polymerases leaving Polκ as the only present Y polymerase (only-κ) and measured DSBs formation. The results obtained with only-κ and siTLS cells were statistically similar, suggesting that while Polκ is extremely relevant, it also needs the participation of other Y family Pols to prevent generation of unscheduled DSBs (Figure 6D).

DISCUSSION

NER is the sole process that effectively removes UV-induced and other bulky helix-distorting lesions in humans. While most NER substrates are rapidly repaired and do not elicit a checkpoint response, a fraction of "problematic" lesions can be generated, where repair synthesis is impeded (Matsumoto et al., 2007). NER can only repair lesions when they are in a double-stranded configuration (Svoboda et al., 1993). COLs, where a UV lesion on one strand is sufficiently close to a second lesion (either UV-induced or pre-existing) on the other strand (Lam and Reynolds, 1986, 1987; Minton and Friedberg, 1974; Novarina et al., 2011; Sedgwick, 1976; Sertic et al., 2012), represent a problem. Indeed, excision of the first adduct leaves in the complementary strand the second lesion, which impedes gap refilling by Polδ, Polε. The gapped intermediate is a natural substrate for both DNA polymerases (refilling) and exonucleases (enlargement). The rate of DNA synthesis by Polδ, Polε is ~20× faster than exonucleolytic processing (Morin et al., 2008), thus the gap is normally closed. In the case of "problematic" lesions, EXO1 nuclease gains a kinetic opportunity to enlarge the gap, generating long ssDNA regions that trigger a checkpoint response alerting the cell of the presence of failed-repair intermediates (Giannattasio et al., 2010; Sertic et al., 2011). In the case of COLs, refilling of the gap, may require the participation of TLS polymerases.

In this work, we investigated the role of Y family TLS polymerases in non-replicating cells, following incision of lesions by NER

Figure 5. TLS Polymerases Prevent the EXO1-Dependent Conversion of UV Lesions into DSBs

(A and B) Serum-starved 48BR cells were silenced for Polκ (k) or luciferase (L), UV irradiated at 20 J/m^2. Protein extracts obtained at the indicated time points were separated by SDS-PAGE and immunoblotted for the indicated proteins.

(C and D) Serum-starved 48BR cells were silenced for Polκ or luciferase, local UV irradiated at 100 J/m^2, and incubated for 5 hr. Fixed cells were immunostained with p-DNA-PK ser2056 antibody (C). Arrowheads indicate p-DNA-PK foci. The graph (D) shows the percentage of cells positive for p-DNA-PK LUDs. Two independent experiments were performed. Error bars, ±SEM.

(E and F) Serum-starved 48BR cells were silenced for luciferase (L) or RAD18 (R)in (E), and for luciferase, RED18, EXO1 (E), or for both RAD18 and EXO1 (R+E) in (F), as indicated. UV-irradiation was performed at 20 J/m^2 and cells were incubated for the indicated time points. Protein extracts were loaded on SDS-PAGE and immunoblotted for the indicated proteins.

(G and H) Before UV-treatment, 48BR cells were silenced for the indicated protein and serum starved. UV irradiation was performed at 100 J/m^2 through 5 μm Isopore filter, using the same procedure as in Figures 1, 2, and 3. Immunofluorescence was performed against p-DNA-PKser2056 5 hr after UV. Representative images are shown (G). The graph (H) reports the percentage of cells positive for p-DNA-PK ser2056 LUDs. 250–300 cells were scored derived from at least two independent experiments. Error bars, ±SEM.

(I) 48BR human primary fibroblasts were serum-starved and silenced for the indicated protein. UV-irradiation was performed at 20 J/m^2 and cells were incubated for 5 hr. Bleocin treatment was used as positive control for DSBs formation. Cells were processed for Neutral Comet Assay. Representative SYBR GREEN stained DNA is shown in the left panel. Tail moment was measured for two independent experiments and four different electrophoretic runs. At least 60 comets were quantified for each sample. The graph to the left reports the distribution of the tail moment. Error bars, ±SEM. From Student's t test: ****p value < 0.0001. ns, not statistically significant.

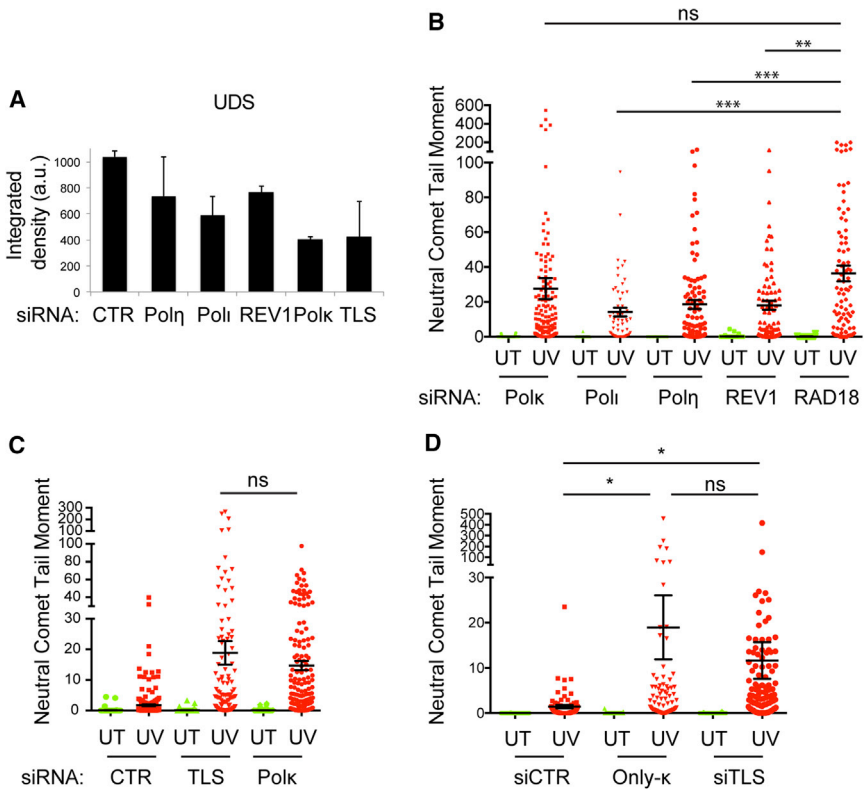

Figure 6. Contribution of Each Y Family TLS Polymerase to UDS and DSBs Formation

(A) Primary cells were UV-irradiated (20 J/m2) and incubated for 2 hr in the presence of EdU. After Click-IT reaction, images were acquired to reach 100 cells for two independent experiments.

(B–D) 48BR primary fibroblasts were serum starved and silenced for the indicated gene. 72 hr post serum-starvation, cells were UV-irradiated (20 J/m^2 + 5 hr incubation) and harvested for Neutral Comet Assay. In (B), we silenced individual TLS polymerases or Rad18. In (C), we silenced Polκ or we simultaneously silenced all Y family enzymes (TLS). In (D), we simultaneously silenced for Polη, Polι, and REV1 (only-κ), or for all Y family enzymes (siTLS).

UT, untreated; UV, UV irradiated. Two independent experiments were performed for each genetic condition. Student's t test was performed: *p value < 0.05; **p value < 0.005; ***p value < 0.0005; ****p value < 0.0001; ns, not statistically significant. Error bars, ±SEM.

factors and the coordination between TLS-dependent gap refilling and EXO1-dependent gap processing. EXO1 acts only at "problematic" UV-induced lesions (e.g., COLs) where its recruitment is dependent upon NER activity (Sertic et al., 2011). Similarly, DNA polymerase κ accumulation at LUDs also requires NER factors (Ogi et al., 2010). We report that Polκ and Polι only accumulate at LUDs where EXO1 is also present, while they are absent in EXO1-negative LUDs. Using EXO1 KO cells, we demonstrated that their recruitment to LUDs is abolished if EXO1 is absent. Recruitment of TLS polymerases may depend upon a physical contact with EXO1 or may be due to the catalytic processing of the gapped intermediate that generates a TLS substrate. Our data show that the mere presence of EXO1 is not sufficient, and recruitment of DNA polymerases κ and ι at LUDs requires the catalytic activity of EXO1. A possible explanation is that by enlarging the original NER-dependent gap, EXO1 exposes other lesions present on the template strand requiring Polκ and Polι activities for repair synthesis of the damaged gaps. Another possibility is that these Y family polymerases are recruited when longer RPA-covered ssDNA stretches are formed, in accordance with observations that Rad18 is preferentially recruited through interactions with RPA (Davies et al., 2008; Huttner and Ulrich, 2008). On the other hand, the other two members of the Y family, Polη and REV1, are still located at LUDs even in EXO1 KO clones, although Polη recruitment was mildly reduced in one of the clones. Recent studies have shown that in S phase Polη has also a non-catalytic role in stabilizing PCNA-monoUb and facilitating loading of other TLS polymerases (Durando et al., 2013). Similarly, REV1 can also play a more structural role, for instance by modulating RAD18 function and promoting PCNA mono-ubiquitylation (Wang et al., 2016).

Interestingly, when normal repair DNA synthesis is impeded, the recruitment of all Y family polymerases at LUDs is enhanced, similarly to what was reported for EXO1 (Sertic et al., 2011). EXO1-positive LUDs (containing the "problematic" lesions) also contain lesions that do not stimulate EXO1 function, so within the EXO1-positive LUDs, some Polη and REV1 will be recruited in an EXO1-dependend manner, while other molecules will be recruited in an EXO1-independent manner. By increasing the UV dose or blocking repair synthesis, the level of ubiquitylated PCNA increases, leading to increased recruitment of all Y family polymerases. These observations suggest that while Polη and REV1 have a more diffused role following UV irradiation (e.g., translesion synthesis through post-replication repair in replicating cells; non-catalytic roles in promoting lesion bypass), Polκ and Polι are more specific for "problematic" lesions that are also processed by EXO1. Our results are consistent with previous work reporting that this TLS polymerase is responsible for a fraction of unscheduled DNA synthesis in non-cycling cells (Ogi et al., 2010).

If DNA lesions are initially processed by NER but gap refilling cannot be promptly completed, EXO1 activity on the gapped substrate leads to checkpoint activation (Giannattasio et al., 2010; Lindsey-Boltz et al., 2014; Sertic et al., 2011). Downregulation of Polκ, by favoring EXO1-dependent processing of the NER intermediate, results in checkpoint hyperactivation effect, and leads to formation of DSBs in UV-irradiated non-replicating cells, consistently with the hypothesis that this polymerase protects cells experiencing "problematic" UV lesions from the unscheduled conversion of these primary lesions to toxic DSBs.

Our data show that UV irradiation *per se* does not seem to significantly induce DSBs, which represent secondary lesions

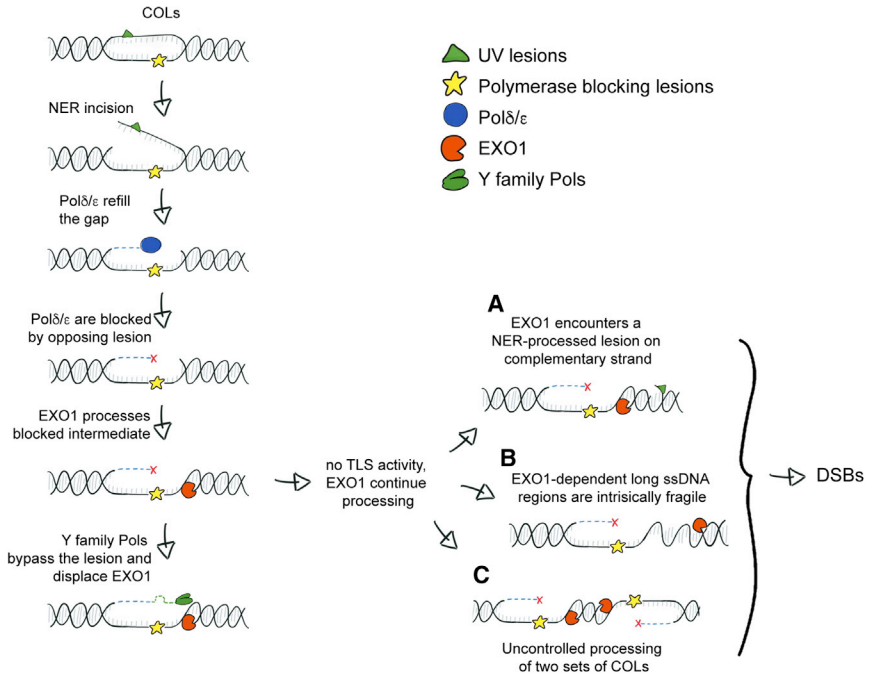

Figure 7. Model for Coordinated Action of TLS Polymerases and EXO1 Activity in the Processing of Problematic UV Lesions

Chromosomes sustain elevated levels of DNA damage on either DNA strands. Following UV irradiation, NER starts processing a UV-induced lesion on one strand; if, during gap refilling, replicative DNA polymerases (Polδ/Polε) encounter an obstacle on the template strand, they fail to complete repair synthesis, and EXO1 has the opportunity to enlarge the gap generating long ssDNA regions, which trigger the DDR. Y family TLS polymerases are crucial to overcome the obstacle on the template strand and are recruited at these intermediates. Bypass of the blockage by Y family TLS polymerases allows gap refilling, quenching of the DDR signal, and prevents further action of EXO1. Loss of the coordination between TLS activities and EXO1 can result in excessive EXO1-dependent processing leading to the formation of unscheduled cytotoxic DSBs. We present three possibilities as sources of DSBs, although others may be possible.

(A) DSBs generated when EXO1 encounters a canonically NER-processed lesion on the opposite strand.

(B) DSBs derived from fragility and breakage of EXO1-dependent long ssDNA regions.

(C) DSBs produced when two COLs are simultaneously processed as described in the text. EXO1 enzymes acting on both antiparallel strands lead to formation of DSBs.

produced as a consequence of repair synthesis problems. In this context, DSBs may arise from DNA breakage within the persisting ssDNA gap or they may be due to the activity of EXO1 that, in the absence of an efficient refilling, can converge onto another repair intermediate, generating a DSB. Strikingly, all the UV-dependent DSBs observed in siRAD18 cells are abolished by downregulating EXO1. Although we cannot exclude that by greatly enlarging the ssDNA gap EXO1 may increase the chance of a stochastic breakage, our data strongly suggest that TLS activity protects non-S phase cells experiencing "problematic" lesions from the formation of unscheduled DSBs. Our results provide a molecular explanation for previous observations of the formation of DSBs following UV irradiation in non-cycling primary fibroblasts (Wakasugi et al., 2014).

The question remaining is whether COLs are part of the "problematic" lesions processed by EXO1, Polκ, and Polι. Although we do not have a definitive answer, our data strongly point toward COLs being the lesions that are responsible for DDR activation and for cytotoxic DSB formation. This view is consistent with an elegant genetic study that shows that G_0 yeast cells do not accumulate two-strand mutations after UV treatment if they lack RAD18 or express a PCNA mutated in K164 (Kozmin and Jinks-Robertson, 2013). Altogether, these results indicate that TLS polymerases are involved in NER-dependent repair synthesis outside of S phase, in addition to their well-described function in PRR in replicating cells.

The work presented here also reveals a separation of roles for different TLS polymerases. While only Polη and REV1 seem to be present at EXO1-negative LUDs, all Y family TLS polymerases are recruited at EXO1-positive UV-damage sites, but only for Polκ and Polι is the recruitment EXO1-dependent (Figures 1 and 2). Polη and REV1 have been reported to act non-catalytically in the stabilization of PCNA mono-ubiquitylation (Durando et al., 2013; Guo et al., 2003; Wang et al., 2016); this would enhance the recruitment of other TLS polymerases. Polκ and Polι are recruited when, during the enlargement of the gap, EXO1 exposes different types of lesions on the ssDNA template strand complexed with RPA. In this view, it is worth noting that Polι efficiently bypasses 6-4PP, abasic sites, and 8-oxo-dG but is not effective at further extending the DNA chain, which is a prerogative of Polκ (Vaisman et al., 2001; Vasquez-Del Carpio et al., 2011; Washington et al., 2002). Moreover, Polκ, on the other hand, can bypass and extend a DNA chain over a variety of other lesions (Avkin et al., 2004; Ohashi et al., 2000; Zhang et al., 2000).

A subsequent analysis of the role of the single TLS in our conditions revealed that Polη, Polι, and REV1 do partly contribute to both UDS and DSB prevention, albeit with a certain degree of redundancy. We suggest that the extent of their participation may depend upon the type of lesions encountered on the template strand during repair synthesis after UV-treatment.

To explain all these results, we propose that the lesion present on the template strand during NER-dependent repair synthesis could be of a broader nature than previously thought (Figure 7). In the past, Lam and Reynolds (1987) provided an accurate calculation of the possible accumulation of closely spaced UV-induced lesions that, depending on the UV-dose used (between 40 and 100 J/m^2 in our experimental setting), represents a fraction of lesions between 0.5% to 1.25%. If we consider the possible presence of a broader

range of lesions (not limited to UV-induced CPDs or 6-4PP) on the template strand, these percentages will greatly increase.

In this situation, a tight balance between TLS polymerase and exonuclease activities is of paramount importance to allow prompt signaling to activate the DDR, complete repair synthesis of damaged templates, and preventing the conversion of "problematic" lesions into DSBs and activation of cell death pathways, to ensure viability of non-proliferating cells. In this scenario, transient inhibition of EXO1 or hyperactivation of TLS polymerases at damage sites could promote cell survival in post-mitotic and terminally differentiated cells exposed to genotoxic agents. Cancer treatment, while aimed at highly replicating cells, also negatively affects non-S phase healthy cells. Furthermore, our work together with a recent report by Janel-Bintz et al. (2017) may provide a mechanistic insight explaining the elevated mutagenesis observed following NER activation, which can promote tumor development and may lead to chemotherapy-induced mutagenesis. Modulations of the mechanism described in this work may have a strong impact on the outcome of cancer therapy.

STAR★METHODS

Detailed methods are provided in the online version of this paper and include the following:

- KEY RESOURCES TABLE
- CONTACT FOR REAGENT AND RESOURCE SHARING
- EXPERIMENTAL MODEL AND SUBJECT DETAILS
  - Cell Lines
- METHOD DETAILS
  - cDNA and siRNA transfection
  - Global and Local UV irradiation
  - Immunofluorescence
  - Unscheduled DNA Synthesis (UDS)
  - FACS analysis
  - Neutral comet assay
  - Total RNA extraction and retrotranscription
  - Semiquantitative PCR
  - Generation of MRC5VI EXO1$^{-/-}$ cell lines
  - Immunoprecipitation
  - Immunoblotting
- QUANTIFICATION AND STATISTICAL ANALYSIS

SUPPLEMENTAL INFORMATION

Supplemental Information includes six figures and one table and can be found with this article online at https://doi.org/10.1016/j.molcel.2018.02.017.

ACKNOWLEDGMENTS

The authors would like to thank Rick Wood and Stefano Ferrari for antibodies; Tomoo Ogi, Alan R. Lehmann, Matthew Jones, Federica Marini, and Simone Sabbioneda for constructs; and Alan R. Lehmann for 48BR primary cells. We also acknowledge Luana Fioriti for her help with the Confocal Microscope. We are thankful to Dr. Federico Lazzaro and Prof. Paolo Plevani for constructive suggestions and critical reading and to all members of our lab for discussions. S.S. was partially supported by a Fondazione Umberto Veronesi (FUV) Fellowship. Work in M.M.-F.'s lab is funded by AIRC (15631), Telethon (GGP15227), and MIUR. Work in A.A.'s lab is funded by Spanish Ministry of Economy and Competitiveness (BFU2016-75058-P).

AUTHOR CONTRIBUTIONS

Investigation, S.S., I.C., A.M., E.T., and S.R.; Conceptualization, S.S. and M.M.-F.; Writing – Original Draft, S.S.; Writing – Review & Editing, A.A. and M.M.-F.; Funding Acquisition, A.A. and M.M.-F.

DECLARATION OF INTERESTS

The authors declare no competing interests.

Received: July 27, 2017
Revised: December 18, 2017
Accepted: February 8, 2018
Published: March 15, 2018; corrected online: April 5, 2018

REFERENCES

Andersen, P.L., Xu, F., and Xiao, W. (2008). Eukaryotic DNA damage tolerance and translesion synthesis through covalent modifications of PCNA. Cell Res. *18*, 162–173.

Avkin, S., Goldsmith, M., Velasco-Miguel, S., Geacintov, N., Friedberg, E.C., and Livneh, Z. (2004). Quantitative analysis of translesion DNA synthesis across a benzo[a]pyrene-guanine adduct in mammalian cells: the role of DNA polymerase kappa. J. Biol. Chem. *279*, 53298–53305.

Bienko, M., Green, C.M., Crosetto, N., Rudolf, F., Zapart, G., Coull, B., Kannouche, P., Wider, G., Peter, M., Lehmann, A.R., et al. (2005). Ubiquitin-binding domains in Y-family polymerases regulate translesion synthesis. Science *310*, 1821–1824.

Bregenhorn, S., and Jiricny, J. (2014). Biochemical characterization of a cancer-associated E109K missense variant of human exonuclease 1. Nucleic Acids Res. *42*, 7096–7103.

Chen, B.P., Chan, D.W., Kobayashi, J., Burma, S., Asaithamby, A., Morotomi-Yano, K., Botvinick, E., Qin, J., and Chen, D.J. (2005). Cell cycle dependence of DNA-dependent protein kinase phosphorylation in response to DNA double strand breaks. J. Biol. Chem. *280*, 14709–14715.

Cooper, P.K., and Hanawalt, P.C. (1972). Heterogeneity of patch size in repair replicated DNA in Escherichia coli. J. Mol. Biol. *67*, 1–10.

Cruet-Hennequart, S., Coyne, S., Glynn, M.T., Oakley, G.G., and Carty, M.P. (2006). UV-induced RPA phosphorylation is increased in the absence of DNA polymerase η and requires DNA-PK. DNA Repair (Amst.) *5*, 491–504.

Davies, A.A., Huttner, D., Daigaku, Y., Chen, S., and Ulrich, H.D. (2008). Activation of ubiquitin-dependent DNA damage bypass is mediated by replication protein a. Mol. Cell *29*, 625–636.

Durando, M., Tateishi, S., and Vaziri, C. (2013). A non-catalytic role of DNA polymerase η in recruiting Rad18 and promoting PCNA monoubiquitination at stalled replication forks. Nucleic Acids Res. *41*, 3079–3093.

El-Shemerly, M., Janscak, P., Hess, D., Jiricny, J., and Ferrari, S. (2005). Degradation of human exonuclease 1b upon DNA synthesis inhibition. Cancer Res. *65*, 3604–3609.

Friedberg, E.C. (2001). Nucleotide excision repair in eukaryotes. eLS. https://doi.org/10.1038/npg.els.0000562.

Giannattasio, M., Lazzaro, F., Siede, W., Nunes, E., Plevani, P., and Muzi-Falconi, M. (2004). DNA decay and limited Rad53 activation after liquid holding of UV-treated nucleotide excision repair deficient S. cerevisiae cells. DNA Repair (Amst.) *3*, 1591–1599.

Giannattasio, M., Follonier, C., Tourrière, H., Puddu, F., Lazzaro, F., Pasero, P., Lopes, M., Plevani, P., and Muzi-Falconi, M. (2010). Exo1 competes with repair synthesis, converts NER intermediates to long ssDNA gaps, and promotes checkpoint activation. Mol. Cell *40*, 50–62.

Goodman, M.F., and Woodgate, R. (2013). Translesion DNA polymerases. Cold Spring Harb. Perspect. Biol. *5*, a010363.

Guo, C., Fischhaber, P.L., Luk-Paszyc, M.J., Masuda, Y., Zhou, J., Kamiya, K., Kisker, C., and Friedberg, E.C. (2003). Mouse Rev1 protein interacts with multiple DNA polymerases involved in translesion DNA synthesis. EMBO J. *22*, 6621–6630.

Guo, C., Kosarek-Stancel, J.N., Tang, T.-S., and Friedberg, E.C. (2009). Y-family DNA polymerases in mammalian cells. Cell. Mol. Life Sci. *66*, 2363–2381.

Harper, J.W., and Elledge, S.J. (2007). The DNA damage response: ten years after. Mol. Cell *28*, 739–745.

Hoege, C., Pfander, B., Moldovan, G.L., Pyrowolakis, G., and Jentsch, S. (2002). RAD6-dependent DNA repair is linked to modification of PCNA by ubiquitin and SUMO. Nature *419*, 135–141.

Huttner, D., and Ulrich, H.D. (2008). Cooperation of replication protein A with the ubiquitin ligase Rad18 in DNA damage bypass. Cell Cycle *7*, 3629–3633.

Janel-Bintz, R., Napolitano, R.L., Isogawa, A., Fujii, S., and Fuchs, R.P. (2017). Processing closely spaced lesions during Nucleotide Excision Repair triggers mutagenesis in E. coli. PLoS Genet. *13*, e1006881.

Kannouche, P.L., and Lehmann, A.R. (2004). Ubiquitination of PCNA and the polymerase switch in human cells. Cell Cycle *3*, 1011–1013.

Kannouche, P., Broughton, B.C., Volker, M., Hanaoka, F., Mullenders, L.H., and Lehmann, A.R. (2001). Domain structure, localization, and function of DNA polymerase eta, defective in xeroderma pigmentosum variant cells. Genes Dev. *15*, 158–172.

Köberle, B., Roginskaya, V., and Wood, R.D. (2006). XPA protein as a limiting factor for nucleotide excision repair and UV sensitivity in human cells. DNA Repair (Amst.) *5*, 641–648.

Kozmin, S.G., and Jinks-Robertson, S. (2013). The mechanism of nucleotide excision repair-mediated UV-induced mutagenesis in nonproliferating cells. Genetics *193*, 803–817.

Lam, L.H., and Reynolds, R.J. (1986). Repair of closely opposed cyclobutyl pyrimidine dimers in UV-sensitive human diploid fibroblasts. Mutat. Res. *166*, 199–205.

Lam, L.H., and Reynolds, R.J. (1987). DNA sequence dependence of closely opposed cyclobutyl pyrimidine dimers induced by UV radiation. Mutat. Res. *178*, 167–176.

Lehmann, A.R. (2003). DNA repair-deficient diseases, xeroderma pigmentosum, Cockayne syndrome and trichothiodystrophy. Biochimie *85*, 1101–1111.

Limsirichaikul, S., Niimi, A., Fawcett, H., Lehmann, A., Yamashita, S., and Ogi, T. (2009). A rapid non-radioactive technique for measurement of repair synthesis in primary human fibroblasts by incorporation of ethynyl deoxyuridine (EdU). Nucleic Acids Res. *37*, e31.

Lindsey-Boltz, L.A., Kemp, M.G., Reardon, J.T., DeRocco, V., Iyer, R.R., Modrich, P., and Sancar, A. (2014). Coupling of human DNA excision repair and the DNA damage checkpoint in a defined in vitro system. J. Biol. Chem. *289*, 5074–5082.

Ma, M., Ye, A.Y., Zheng, W., and Kong, L. (2013). A guide RNA sequence design platform for the CRISPR/Cas9 system for model organism genomes. BioMed Res. Int. *2013*, 270805.

Marini, F., Kim, N., Schuffert, A., and Wood, R.D. (2003). POLN, a nuclear PolA family DNA polymerase homologous to the DNA cross-link sensitivity protein Mus308. J. Biol. Chem. *278*, 32014–32019.

Marini, F., Nardo, T., Giannattasio, M., Minuzzo, M., Stefanini, M., Plevani, P., and Muzi Falconi, M. (2006). DNA nucleotide excision repair-dependent signaling to checkpoint activation. Proc. Natl. Acad. Sci. USA *103*, 17325–17330.

Marti, T.M., Hefner, E., Feeney, L., Natale, V., and Cleaver, J.E. (2006). H2AX phosphorylation within the G1 phase after UV irradiation depends on nucleotide excision repair and not DNA double-strand breaks. Proc. Natl. Acad. Sci. USA *103*, 9891–9896.

Matsumoto, M., Yaginuma, K., Igarashi, A., Imura, M., Hasegawa, M., Iwabuchi, K., Date, T., Mori, T., Ishizaki, K., Yamashita, K., et al. (2007). Perturbed gap-filling synthesis in nucleotide excision repair causes histone H2AX phosphorylation in human quiescent cells. J. Cell Sci. *120*, 1104–1112.

Minton, K., and Friedberg, E.C. (1974). Letter: Evidence for clustering of pyrimidine dimers on opposite strands of U.V.-irradiated bacteriophage DNA. Int. J. Radiat. Biol. Relat. Stud. Phys. Chem. Med. *26*, 81–85.

Morin, I., Ngo, H.-P., Greenall, A., Zubko, M.K., Morrice, N., and Lydall, D. (2008). Checkpoint-dependent phosphorylation of Exo1 modulates the DNA damage response. EMBO J. *27*, 2400–2410.

Muniandy, P.A., Liu, J., Majumdar, A., Liu, S.T., and Seidman, M.M. (2010). DNA interstrand crosslink repair in mammalian cells: step by step. Crit. Rev. Biochem. Mol. Biol. *45*, 23–49.

Novarina, D., Amara, F., Lazzaro, F., Plevani, P., and Muzi-Falconi, M. (2011). Mind the gap: keeping UV lesions in check. DNA Repair (Amst.) *10*, 751–759.

O'Driscoll, M., and Jeggo, P.A. (2003). Clinical impact of ATR checkpoint signalling failure in humans. Cell Cycle *2*, 194–195.

Ogi, T., and Lehmann, A.R. (2006). The Y-family DNA polymerase kappa (pol kappa) functions in mammalian nucleotide-excision repair. Nat. Cell Biol. *8*, 640–642.

Ogi, T., Limsirichaikul, S., Overmeer, R.M.R.M., Volker, M., Takenaka, K., Cloney, R., Nakazawa, Y., Niimi, A., Miki, Y., Jaspers, N.G., et al. (2010). Three DNA polymerases, recruited by different mechanisms, carry out NER repair synthesis in human cells. Mol. Cell *37*, 714–727.

Ohashi, E., Bebenek, K., Matsuda, T., Feaver, W.J., Gerlach, V.L., Friedberg, E.C., Ohmori, H., and Kunkel, T.A. (2000). Fidelity and processivity of DNA synthesis by DNA polymerase kappa, the product of the human DINB1 gene. J. Biol. Chem. *275*, 39678–39684.

Overmeer, R.M.R.M., Moser, J., Volker, M., Kool, H., Tomkinson, A.E., van Zeeland, A.A., Mullenders, L.H.F., and Fousteri, M. (2011). Replication protein A safeguards genome integrity by controlling NER incision events. J. Cell Biol. *192*, 401–415.

Sabbioneda, S., Gourdin, A.M., Green, C.M., Zotter, A., Giglia-Mari, G., Houtsmuller, A., Vermeulen, W., and Lehmann, A.R. (2008). Effect of proliferating cell nuclear antigen ubiquitination and chromatin structure on the dynamic properties of the Y-family DNA polymerases. Mol. Biol. Cell *19*, 5193–5202.

Sale, J.E., Lehmann, A.R., and Woodgate, R. (2012). Y-family DNA polymerases and their role in tolerance of cellular DNA damage. Nat. Rev. Mol. Cell Biol. *13*, 141–152.

Sanjana, N.E., Shalem, O., and Zhang, F. (2014). Improved vectors and genome-wide libraries for CRISPR screening. Nat. Methods *11*, 783–784.

Sarkar, S., Davies, A.A., Ulrich, H.D., and McHugh, P.J. (2006). DNA interstrand crosslink repair during G1 involves nucleotide excision repair and DNA polymerase zeta. EMBO J. *25*, 1285–1294.

Schärer, O.D. (2013). Nucleotide excision repair in eukaryotes. Cold Spring Harb. Perspect. Biol. *5*, a012609.

Sedgwick, S.G. (1976). Misrepair of overlapping daughter strand gaps as a possible mechanism for UV induced mutagenesis in UVR strains of Escherichia coli: a general model for induced mutagenesis by misrepair (SOS repair) of closely spaced DNA lesions. Mutat. Res. *41*, 185–200.

Sertic, S., Pizzi, S., Cloney, R., Lehmann, A.R., Marini, F., Plevani, P., and Muzi-Falconi, M. (2011). Human exonuclease 1 connects nucleotide excision repair (NER) processing with checkpoint activation in response to UV irradiation. Proc. Natl. Acad. Sci. USA *108*, 13647–13652.

Sertic, S., Pizzi, S., Lazzaro, F., Plevani, P., and Muzi-Falconi, M. (2012). NER and DDR: classical music with new instruments. Cell Cycle *11*, 668–674.

Sertic, S., Evolvi, C., Tumini, E., Plevani, P., Muzi-Falconi, M., and Rotondo, G. (2013). Non-canonical CRL4A/4B(CDT2) interacts with RAD18 to modulate post replication repair and cell survival. PLoS ONE *8*, e60000.

Sertic, S., Roma, S., Plevani, P., Lazzaro, F., and Muzi-Falconi, M. (2018). Study of UV-induced DNA Repair Factor Recruitment: Kinetics and Dynamics. Methods Mol. Biol. *1672*, 101–105.

Shalem, O., Sanjana, N.E., Hartenian, E., Shi, X., Scott, D.A., Mikkelson, T., Heckl, D., Ebert, B.L., Root, D.E., Doench, J.G., and Zhang, F. (2014). Genome-scale CRISPR-Cas9 knockout screening in human cells. Science *343*, 84–87.

Singh, R., Kuscu, C., Quinlan, A., Qi, Y., and Adli, M. (2015). Cas9-chromatin binding information enables more accurate CRISPR off-target prediction. Nucleic Acids Res. *43*, e118.

Spivak, G. (2015). Nucleotide excision repair in humans. DNA Repair (Amst.) *36*, 13–18.

Svetlova, M., Solovjeva, L., Pleskach, N., Yartseva, N., Yakovleva, T., Tomilin, N., and Hanawalt, P. (2002). Clustered sites of DNA repair synthesis during early nucleotide excision repair in ultraviolet light-irradiated quiescent human fibroblasts. Exp. Cell Res. *276*, 284–295.

Svoboda, D.L., Smith, C.A., Taylor, J.S., and Sancar, A. (1993). Effect of sequence, adduct type, and opposing lesions on the binding and repair of ultraviolet photodamage by DNA photolyase and (A)BC excinuclease. J. Biol. Chem. *268*, 10694–10700.

Tran, P.T., Erdeniz, N., Symington, L.S., and Liskay, R.M. (2004). EXO1-A multi-tasking eukaryotic nuclease. DNA Repair (Amst.) *3*, 1549–1559.

Vaisman, A., and Woodgate, R. (2017). Translesion DNA polymerases in eukaryotes: what makes them tick? Crit. Rev. Biochem. Mol. Biol. *52*, 274–303.

Vaisman, A., Tissier, A., Frank, E.G., Goodman, M.F., and Woodgate, R. (2001). Human DNA polymerase iota promiscuous mismatch extension. J. Biol. Chem. *276*, 30615–30622.

Vasquez-Del Carpio, R., Silverstein, T.D., Lone, S., Johnson, R.E., Prakash, L., Prakash, S., and Aggarwal, A.K. (2011). Role of human DNA polymerase κ in extension opposite from a cis-syn thymine dimer. J. Mol. Biol. *408*, 252–261.

Volker, M., Moné, M.J., Karmakar, P., van Hoffen, A., Schul, W., Vermeulen, W., Hoeijmakers, J.H., van Driel, R., van Zeeland, A.A., and Mullenders, L.H. (2001). Sequential assembly of the nucleotide excision repair factors in vivo. Mol. Cell *8*, 213–224.

Wakasugi, M., Sasaki, T., Matsumoto, M., Nagaoka, M., Inoue, K., Inobe, M., Horibata, K., Tanaka, K., and Matsunaga, T. (2014). Nucleotide excision repair-dependent DNA double-strand break formation and ATM signaling activation in mammalian quiescent cells. J. Biol. Chem. *289*, 28730–28737.

Wang, Z., Huang, M., Ma, X., Li, H., Tang, T., and Guo, C. (2016). REV1 promotes PCNA monoubiquitylation through interacting with ubiquitylated RAD18. J. Cell Sci. *129*, 1223–1233.

Washington, M.T., Johnson, R.E., Prakash, L., and Prakash, S. (2002). Human DINB1-encoded DNA polymerase kappa is a promiscuous extender of mispaired primer termini. Proc. Natl. Acad. Sci. USA *99*, 1910–1914.

Williams, H.L., Gottesman, M.E., and Gautier, J. (2012). Replication-independent repair of DNA interstrand crosslinks. Mol. Cell *47*, 140–147.

Zhang, Y., Yuan, F., Wu, X., Wang, M., Rechkoblit, O., Taylor, J.S., Geacintov, N.E., and Wang, Z. (2000). Error-free and error-prone lesion bypass by human DNA polymerase kappa in vitro. Nucleic Acids Res. *28*, 4138–4146.

STAR★METHODS

KEY RESOURCES TABLE

REAGENT or RESOURCE	SOURCE	IDENTIFIER
Antibodies		
GFP	Clontech	632677
p-RPA32 ser4/8	Bethyl Laboratories	A300-245A-M
p-p53ser15	Cell Signaling	9284
XPB	Cell Signaling	8746
PCNA-mUbK164	Cell Signaling	D5C7P
RPA32	Novus Biologicals	NB100-332
p53 (DO1)	Genespin	N/A
Actin	Sigma-Aldrich	A2066
Vinculin	Sigma-Aldrich	V9131
XPA clone 12F5	Köberle et al., 2006	From R. Wood
EXO1 F15	El-Shemerly et al., 2005	From S. Ferrari
γH2AX	Upstate	05-636
H2AX	Upstate	07-627
PCNA (PC10)	SantaCruz Biotechnology	sc-56
RAD18	CusaBio	CSB-PA889102LA01HU
H3	Abcam	ab1791
p-DNA-PK ser2056	Abcam	ab18192
AlexaFluor goat anti-mouse 488	Life Technologies	A28175
AlexaFluor goat anti-rabbit 488	Life Technologies	A-11034
AlexaFluor goat anti-mouse 594	Life Technologies	A-11032
AlexaFluor Goat anti-mouse 647	Life Technologies	A-21235
Bacterial and Virus Strains		
DH5alpha	This paper	N/A
Stbl3	Life Technologies	C737303
Chemicals, Peptides, and Recombinant Proteins		
AraC	Sigma-Aldrich	C1768
Bleocin	Merk	203408
Critical Commercial Assays		
Click-IT Imaging kit AlexFluor594	Life Technologies	C10339
Click-IT Imaging kit AlexFluor488	Life Technologies	C10337
Experimental Models: Cell Lines		
MRC5VI	Ogi et al., 2010	N/A
48BR	Ogi et al., 2010	N/A
XP20PV	Ogi et al., 2010	N/A
MRC5VI LUC	This paper	N/A
MRC5VI EXO1−/−.3	This paper	N/A
MRC5VI EXO1−/−.15	This paper	N/A
XP4BE (XP-V)	From M. Stefanini, IGM-CNR Pavia	N/A
Oligonucleotides		
See Table S1	N/A	N/A
Recombinant DNA		
eGFP-Polη	Sabbioneda et al., 2008	From S. Sabbioneda
eGFP-Polκ	Ogi et al., 2010	From T. Ogi

(*Continued on next page*)

Continued

REAGENT or RESOURCE	SOURCE	IDENTIFIER
eGFP-Polι	Sabbioneda et al., 2008	From A.R. Lehmann
eGFP-REV1	N/A	From M.J. Jones
eGFP-Polν	Marini et al., 2003	From F. Marini
EXO1-mCherry	Sertic et al., 2013	N/A
EXO1-D173A-mCherry	This paper	N/A
pMD2.g	From D. Trono	Addgene-12259
PAX2	From D. Trono	Addgene-12260
lentiCRISPRv2	Sanjana et al., 2014	Addgene-52961
Software and Algorithms		
ImageJ (UDS)	ImageJ Software	N/A
CometScore (Tail moment)	CometScore Software	TriTek
Image Lab (Western Blotting)	Image Lab Software	Bio-Rad
CellQuest (FACS analysis)	Cell Quest Software	BD Bioscience
Other		
UV-Lamp (254 nm)	VL-6.C	11-102475
Isopore membrane filters	Merck	TMTP04700
BD FACScan	BD Biosciences	N/A

CONTACT FOR REAGENT AND RESOURCE SHARING

Text

EXPERIMENTAL MODEL AND SUBJECT DETAILS

Cell Lines

MRC5VI cell line was grown in DMEM containing 10% FBS (Euroclone), 200mM L-Glutammine and Penicillin/Streptomycin solution and held at 37°C in a humidified atmosphere (5% CO2). 48BR, XP20PV (XP-A) and XP4BE primary fibroblasts were cultured in the same medium supplemented with 15% FBS.

Serum starvation, where indicated, was performed for 72h using DMEM supplemented with 0.5% FBS.

METHOD DETAILS

cDNA and siRNA transfection

Cells were seeded and transfected 24-48h after attachment. Cells carrying overexpression constructs were transfected with Lipofectamine3000 (ThermoFisher) following manufacture's instruction. Primary cells depleted for the indicated proteins by siRNA were transfected using HiPerfect (QIAGEN).

Global and Local UV irradiation

For global UV irradiation, culture medium was removed and cells were washed once with PBS and irradiated with a UV-lamp (254 nm) at a dose of 20 J/m^2. Medium was then added back and cells were returned to culture conditions for the indicated times.

Local UV damage was achieved by irradiating cells through a 5 μm Isopore filter (TMTP Merck-Millipore) with a UV-BOX (254 nm wavelength) at a rate between 0.5-0.7 J/m^2/s and a final dose of 40 J/m^2 or 100 J/m^2 (Sertic et al., 2018).

Immunofluorescence

Cells were seeded on coverslips, transfected and irradiated as described above. Cells were washed once in PBS, fixed 20 min with 2% paraformaldehyde in PBS and permeabilized for 5 min with ice cold PBS containing 0.5% Triton X-100. Blocking was performed in 10% BSA in PBS for at least 30 min; the solution was subsequently replaced with primary Abs diluted in PBS with 0.1% TWEEN 20 (PBST) for 2 h at room temperature. Coverslips were washed three times in PBST for 5-10 min and secondary antibodies diluted in PBST (1:1000) were added. Cells were rinsed in PBST three times for 10 min and mounted using ProLong Gold with DAPI (Invitrogen). Images were taken using a widefield Leica DMRA2 Microscope (Leica FW4000 software) with 100X oil immersion objective (1.30 N.A.) or a Leica SPE confocal Microscope with 63X oil immersion objective. Percentage of the indicated proteins' positive LUDs were scored counting XPA or XPB accumulation at local damage only in the transfected cells; 1 was assigned every time

tagged-proteins showed accumulation at local damage and 0 when it was absent. At least 30-40 LUDs were scored for each independent experiment and at least 3 independent experiments were performed for each condition, unless otherwise specified in the Figure legend.

EdU detection was achieved by using a Click-IT imaging kit (LifeTechnologies) AlexaFluor488.

Unscheduled DNA Synthesis (UDS)

Cells were washed with PBS, followed by irradiation with 20 J/m^2 of UVC (254nm). After UV irradiation, cells were immediately incubated with serum-free DMEM supplemented with 10 μM EdU. Fixation was carried out using 3.7% formaldehyde for 15 min. After washing with 3% BSA in PBS, cells were permeabilized with 0.5% Triton X-100 in PBS for 20 min. Incorporated EdU was detected by fluorescent azide coupling reaction according to the manufacturer instruction (Click-IT).

Cells were captured with a fluorescent microscope (Leica-DMRA2-40X objective) equipped with a CCD camera, and images were processed and analyzed with ImageJ Software. At least 100 G_0 cells were randomly selected, and the average nuclear fluorescent intensity was calculated and normalized for the background.

FACS analysis

Cells were harvested by tripsinization and washed in PBS, fixed in 70% ice cold EtOH and stored at 4°C over night. Cells were washed with 1% BSA/PBS and stained with propidium iodide solution (20 ug/ml-Sigma Aldrich P4864, RNaseA 10 ug/mL Sigma-Aldrich R6513) at room temperature for 30 min. FACS analyses were performed on a BD FACScan and quantified with Cell Quest software (BD Bioscience). 10^4 events were acquired and the same number is visualized in the histograms.

Neutral comet assay

Cells were harvested and processed as indicated in Trevigen Comet Assay protocol following manufacturer's instruction (Appendix). Briefly, 10^5 cells/ml were embedded 1:10 into low melting agarose and covered by lysis buffer for 30' on ice and in the dark. Coverslips were immersed into TBE 1X and electrophoresis was applied at 1V per cm for 15' in a cold room, on ice and in the dark. DNA was stained with SYBR Green dye and images were acquired under a Leica DMRA2 Fluorescence Microscope with a 20X objective.

Tail moment was calculated using CometScore (TriTek) by measuring at least 90 events for each experiment.

Total RNA extraction and retrotranscription

Total RNA was isolated using a High Pure RNA isolation kit (Roche) and 0,5 μg of RNA was retrotranscribed using iScript Reverse Transcription Supermix (Bio-Rad) according to manufacturer's protocol.

Semiquantitative PCR

The cDNA product was diluted 1:5 in TE. PCR primers were designed to amplify 100-200 bp fragments. GAPDH was used as housekeeping control. RT-PCR was performed.

Generation of MRC5VI EXO1$^{-/-}$ cell lines

The EXO1 knockout strategy and controls are displayed in Figure S3. Small guide RNAs (sgRNAs) targeting exon 1 of the NG_029100 (1q43) gene were selected using the Cas9 Design tool (Ma et al., 2013), with the sequences in Table S1. sgRNA sequences were purchased as DNA oligonucleotides (Eurofins MWG) and cloned into lentiCRISPRv2 (Addgene) Sanjana et al., 2014; Shalem et al., 2014). MRC5VI cells were infected with lentiCRISPRv2, human codon-optimized Cas9-EXO1+, -EXO1- or vector containing sgRNA against Luciferase as control (LUC), and left to recover for 3 days before addition of selective medium containing 1 μg/ml Puromycin. After 10 days, cells were plated to limiting dilution 1 cell per well using FACSAria sorter and allowed to form colonies from single cells. Genomic DNA (gDNA) from clones was further analyzed by GeneArt Genomic Cleavage Detection kit (LifeTechnologies) according to Manufacturer's indication. gDNA was extracted and purified using a NucleoSpin Tissue kit (Macherey-Nagel) according to the manufacturer's instructions. To amplify targeted locus for GeneArt Genomic Detection kit, primers were used, see Table S1.

Putative off-target of both sgRNAs sequences were scored using the algorithm developed in Singh et al. (2015). Sequences were controlled amplifying the region of interest from gDNA of positive KO clones and sent for Sanger-sequenced. Results from these analyses are shown in Figure S3.

Immunoprecipitation

MRC5VI and MRC5VI EXO1$^{-/-}$ cell lines were cultured up to 80% confluence for 24 h, harvested with PBS and processed as described in El-Shemerly et al. (2005). 1.5 mg protein, determined by the Bradford method, and F15 anti-EXO1 Ab were used for the IPs as described in El-Shemerly et al. (2005).

Immunoblotting

Cells were lysed in 1% SDS sample buffer (62.5 mM Tris-HCl, pH 6.8, 2% SDS, 10% glycerol, 50 mM DTT, 0.01% bromophenol blue), sonicated 10 s, and heated at 95°C for 5 min. Equal amounts of total protein extracts were analyzed by SDS-PAGE. Immunoblots were acquired using BioRad ChemiDoc Touch apparatus (4X4 binning) and subsequently quantified using ImageLab software.

QUANTIFICATION AND STATISTICAL ANALYSIS

Data are expressed as ± standard error of the mean (SEM) unless otherwise stated. Statistical tests were performed using the Student's t test.